Quantum Mechanical Tunneling in Hydrogen Atom Abstraction from Solid Acetonitrile at 77–87°K

by Robert J. Le Roy,*

Department of Physics, University of Toronto, Toronto 181, Ontario, Canada[1]

Estel D. Sprague, and Ffrancon Williams

Department of Chemistry, University of Tennessee, Knoxville, Tennessee[2] *37916* *(Received August 2, 1971)*

Publication costs assisted by the U. S. Atomic Energy Commission

Recent measurements of the rate of H-atom abstraction from solid acetonitrile at 77–87°K yielded an apparent activation energy of 1.4 ± 0.1 kcal/mol, much smaller than the value 10.0 ± 0.5 kcal/mol reported earlier for the same reaction occurring in the gas phase at 373–573°K. However, exact one-dimensional tunneling calculations for potential energy barriers of different sizes and shapes show that the two sets of results may be quantitatively understood in terms of a single gaussian-shaped potential barrier. This means that at 77–87°K the reaction proceeds almost totally *via* quantum-mechanical tunneling.

1. Introduction

In certain theories of chemical reaction rates it is customary to treat the reacting system as a mass point moving on a potential energy surface from a region labeled "reagents" to one labeled "products."[3–5] A widely used simplified version of this approach treats the reaction as the motion of the mass point along a critical one-dimensional "reaction-coordinate" on the potential surface. Although the potential surface is in general multidimensional, this one-dimensional approach has received a great deal of attention, probably largely because of its simplicity. However, it does intuitively seem reasonably appropriate for describing reactions such as the transfer of hydrogenic atoms between relatively massive chemical groups, where steric factors could effectively exclude all but a very limited set of "reaction paths."

It has been evident for some time that studies of hydrogen atom reactions at very low temperatures should provide particularly useful tests of simple theories of chemical reaction rates.[3–5] However, sundry experimental difficulties have severely restricted the availability of reliable data. Although there have been reports[6,7] of hydrogen atom abstraction from neutral molecules by free radicals or radical ions at 77°K, the process has usually been inferred only from the final observation of radicals whose origin can be rationalized in this way. Also, the possible intervention of "hot-radical" processes in photochemistry and radiation chemistry can usually provide alternate explanations for the occurrence at low temperatures of reactions whose activation energies (measured at high temperatures) exceed 5 kcal/mol.[6,7] In contrast, the recent report[8] of hydrogen atom abstraction by methyl radicals in solid γ-irradiated acetonitrile at low temperatures

$$\cdot CH_3 + CH_3CN \longrightarrow CH_4 + \cdot CH_2CN \qquad (1)$$

is unique in two ways. First, the hydrogen atom abstraction mechanism was established kinetically by showing that the decay of $\cdot CH_3$ *and* the appearance of $\cdot CH_2CN$ occur with the same rate constant. Moreover, the linear variation of this rate constant with the number of H atoms in partially deuterated acetonitriles demonstrates the expected very large primary kinetic isotope effect. Second, since the methyl radicals are produced by photobleaching γ-irradiated acetonitrile with visible light, their subsequent thermal decay can be followed either in the dark or during continuous photobleaching of the sample. Essentially the same rate constant was obtained in each case, which necessarily eliminates possible contributions from hot-radical reactions.

In the following, these provocative new data will be analyzed in terms of the above one-dimensional

(1) Supported by the National Research Council of Canada. The work was initiated while this author was at the Theoretical Chemistry Institute, University of Wisconsin, Madison, Wisconsin, and was at that time supported by National Science Foundation Grant GB-16665.

(2) Work supported by U. S. Atomic Energy Commission Contract No. AT-(40-1)-2968; this is AEC Document No. ORO-2968-64.

(3) (a) R. P. Bell, *Proc. Roy. Soc. Ser. A*, **148**, 241 (1935); (b) S. Glasstone, K. J. Laidler, and H. Eyring, "The Theory of Rate Processes," McGraw-Hill, New York, N. Y., 1941.

(4) (a) R. P. Bell, *Trans. Faraday Soc.*, **55**, 1 (1959); (b) "The Proton in Chemistry," Cornell University Press, Ithaca, New York, 1959, Chapter 11; (c) H. S. Johnston, "Gas Phase Reaction Rate Theory," Ronald Press, New York, N. Y., 1966.

(5) E. F. Caldin, *Chem. Rev.*, **69**, 135 (1969).

(6) J. E. Willard in "Fundamental Processes in Radiation Chemistry," P. Ausloos, Ed., Wiley-Interscience, New York, N. Y., 1968, p 599.

(7) J. E. Bennett, B. Mile, A. Thomas, and B. Ward, *Advan. Phys. Org. Chem.*, **8**, 1 (1970).

(8) E. D. Sprague and F. Williams, *J. Amer. Chem. Soc.*, **93**, 787 (1971).

model. The basic purpose of this treatment is not really to prove or disprove the validity of an obviously oversimplified model. Rather, it is to determine whether this familiar picture which has proved so useful in interpreting reaction rates in the gaseous and liquid state can also provide a consistent interpretation of low-temperature solid-phase results. If this is true, the new low-temperature acetonitrile rate measurements must be compatible with the earlier[9] high-temperature (373–573°K) gas-phase data for this reaction. Within the framework of the model, this would mean that at liquid nitrogen temperatures the reaction must proceed mainly by quantum-mechanical tunneling through the potential barrier.

2. Method of Approach

According to the one-dimensional model, the temperature dependence of the rate constant $k(T)$ may be expressed as

$$k(T) = A\Gamma(T)e^{-V_0/RT} \quad (2)$$

In eq 2, V_0 is the height of the potential barrier on the reaction coordinate, R the gas constant, A the approximately temperature-independent frequency of mass-point collisions with the barrier, and $\Gamma(T)$ is the ratio of the quantum mechanical to the classical barrier transmission rate for a Boltzmann distribution of incident mass-point kinetic energies. At high temperatures $\Gamma(T)$ smoothly approaches unity, and hence the apparent activation energy

$$E_{app} = -R\frac{\mathrm{d}\ \ln\ [k(T)]}{\mathrm{d}(1/T)} = V_0 - R\frac{\mathrm{d}\ \ln\ [\Gamma(T)]}{\mathrm{d}(1/T)} \quad (3)$$

approaches V_0. On the other hand, as the temperature decreases the tunneling factor $\Gamma(T)$ grows at a monotonically increasing rate, and hence at low T, E_{app} will be significantly less than V_0. Thus, as Bell[3a] pointed out in 1935, eq 2 and 3 imply that a significant decrease in E_{app} with decreasing temperature is qualitative evidence of a large contribution from tunneling.

Wijnen's[9] high-temperature (373–573°K) gas-phase measurements of reaction 1 were carried out with deuterated methyl radicals, and had an $E_{app} = 10.0 \pm 0.5$ kcal/mol. In the procedure used here for fitting the experimental data to eq 2, it is assumed that this approximates the high-temperature limit of E_{app}, and hence that $V_0 = 10.0 \pm 0.5$ kcal/mol. The validity of this assumption will be verified below. In the following, tunneling factors will be calculated for a number of different trial potential barriers with heights $V_0 = 10.0 \pm 0.5$ kcal/mol in an attempt to find a barrier which will yield both the magnitude and the temperature dependence of the reported[8] low-temperature 77–87°K rate constants. The experimental temperature dependence is given by[8]

$$E_{app}\ (82°\mathrm{K}) = 1.4 \pm 0.1\ \mathrm{kcal/mol} \quad (4)$$

and its value for a given model barrier may be calculated directly from eq 3 using computed values of $\Gamma(T)$ at $T = 77$ and 87°K.

In order to calculate the absolute value of the rate constant from a computed $\Gamma(T)$ for a given potential barrier, one must first estimate a value for the frequency factor A in eq 2. This quantity cannot be obtained experimentally from the low-temperature solid-phase measurements[8] since it is inextricably coupled to $\Gamma(T)$ in eq 2. Furthermore, use of a gas-kinetic value such as might be suitable in the high-temperature gas-phase case[9] is obviously inappropriate for describing events in the solid. On the other hand, since the reagents are frozen in a crystalline matrix at 77–87°K, the A factor must be directly related to the frequencies of the motion of the hydrogenic atoms in the acetonitrile. Spectroscopic measurements in the solid phase near 77°K show that both the symmetric and antisymmetric CH stretching frequencies are *ca.* 9×10^{13} sec^{-1}.[10] Allowing for some uncertainties due to the possible inclusion of a degeneracy factor or participation of other normal modes, substitution of this A value and the experimental[8] $k(77°\mathrm{K}) = 0.025$ min^{-1} into eq 2 yields

$$\log\ [\Gamma(T)e^{-V_0/RT}]_{77°\mathrm{K}} = \log\ [k(77°\mathrm{K})/A] = -17.5 \pm 0.5 \quad (5)$$

The left-hand side of eq 5 may be readily computed for any chosen model barrier. In the following, the size and shape of the appropriate barrier will be determined by performing calculations for a range of barriers until both eq 4 and 5 are satisfied.

3. Determination of Barrier Size and Shape

In the present work three different types of model potential barriers are considered: Eckart barriers[11]

$$V_E(x) = V_0/\cosh^2\ (x/a) \quad (6)$$

truncated parabolic barriers

$$V_p(x) = V_0[1 - (x/a)^2]\ \text{for}\ |x| < a \quad (7)$$
$$= 0 \qquad \text{for}\ |x| > a$$

and gaussian barriers

$$V_G(x) = V_0e^{-(x/a)^2} \quad (8)$$

For a given choice of values of the parameters V_0 and a, all three types of barriers have the same height and curvature at the maximum, although the corresponding full-widths at half maximum increase from parabolic to gaussian to Eckart. As is customary,[3a,4a,4b,12] the

(9) M. H. J. Wijnen, *J. Chem. Phys.*, **22**, 1074 (1954). In this work, the activation energy of reaction 1 was obtained from an analysis of ratios of rate constants, so the frequency factor A in eq 2 was not an observable.

(10) (a) D. E. Milligan and M. E. Jacox, *J. Mol. Spectrosc.*, **8**, 126 (1962); (b) E. L. Pace and L. J. Noe, *J. Chem. Phys.*, **49**, 5317 (1968).

(11) C. Eckart, *Phys. Rev.*, **35**, 1303 (1930).

(12) R. J. Le Roy, K. A. Quickert, and D. J. Le Roy, *Trans. Faraday Soc.*, **66**, 2997 (1970).

size and width of a given type of barrier will be characterized by V_0 and the dimensionless parameter

$$\beta = \pi a(2\mu V_0)^{1/2}/\hbar = 14.30946a\ [\text{Å}](\mu[\text{amu}]V_0[\text{kcal/mol}])^{1/2} \quad (9)$$

where μ is the effective reduced mass of the reacting system, and a is the length scaling factor appearing in eq 6–8. In the present case, μ is taken as the mass of the hydrogenic atom being abstracted.

While the exact transmission probability of Eckart barriers as a function of incident particle kinetic energy is known analytically,[11] this is not the case for truncated parabolic and gaussian barriers. However, for the latter two, and in fact for any chosen type of one-dimensional barrier, these permeabilities may be readily and accurately computed numerically. Here, this was done using the improved version of the method of ref 12 which is discussed in the Appendix.

For each of V_0 = 9.5, 10.0, and 10.5 kcal/mol, E_{app} (82°K) and log $\{\Gamma(T)\ e^{-V_0/RT}\}_{77°K}$ were calculated for each of the three types of potentials for a range of barrier sizes (*i.e.*, divers β values). The results are the solid curves on Figures 1–3; in each case the horizontal dashed line represents the corresponding experimental quantity and the shaded region its uncertainty. It is evident that eq 4 and 5 can be simultaneously satisfied only for gaussian barriers (Figure 3). At barrier sizes chosen to satisfy eq 5, truncated parabolas give E_{app} (82°K) values which are much too small (Figure 1), while for Eckart barriers the corresponding values are slightly too large (Figure 2). The properties of the barriers corresponding to the labeled points in Figures 1–3 [P_1, E_1, G_1, and G_2] are given in Table I, while the barriers corresponding to points P_1, E_1, and G_1 are shown in Figure 4.

Table I: Properties of Potential Barriers Satisfying Eq 4 and 5

Barrier	β	V_0, kcal/mol	a, Å	log $\{\Gamma(T)e^{-V_0/RT}\}_{77°K}$	E_{app} (82°K), kcal/mol
P_1	42.8	10.5	0.919	−18.0	0.46
E_1	25.6	10.5	0.550	−17.0	1.72
G_1	29.6	10.5	0.636	−17.5	1.40
G_2	29.2	10.0	0.643	−17.2	1.46

Figure 5 shows calculated values of $E_{app}(T)$ and $\Gamma(T)$ for the H- and D-atom abstractions corresponding to gaussian potential barrier G_1 (of course the D-atom results correspond to β = 41.86; see eq 9). It is interesting to note that for H-atom abstraction at 373–573°K, $E_{app} \approx$ 10.0 kcal/mol (*cf.* V_0 = 10.5 kcal/mol), right in the center of the uncertainty in the experimental high-temperature value,[9] 10.0 ± 0.5 kcal/mol.

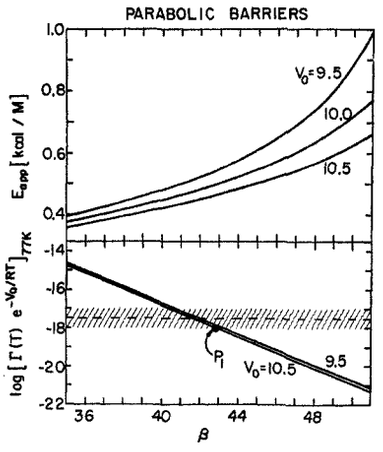

Figure 1. Apparent activation energies E_{app} (82°K) and values of log $[\Gamma(T)\ e^{-V_0/RT}]_{77°K}$ calculated for truncated parabolic barriers (see eq 7) of different sizes (divers β's). The horizontal dashed lines represent the experimental quantities of eq 4 and 5.

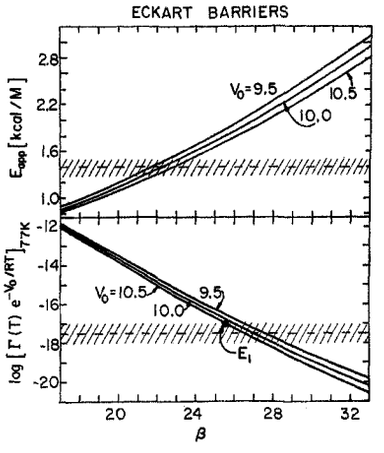

Figure 2. As in Figure 1, for Eckart barriers (see eq 6).

4. Discussion

One apparent inconsistency in the present treatment is the practice of utilizing the quantal vibrational frequencies to estimate the A factor in eq 2, while the tunneling factor calculation assumes a continuous Boltzmann distribution of kinetic energies incident on the potential barrier. Another objection is that the present work has essentially fitted three data:[12a] the high-temperature E_{app}, low-temperature E_{app}, and a low-temperature rate constant, with three parameters:

(12a) Note Added in Proof. Recently, additional esr studies have been carried out on reaction 1 in Crystal I of acetonitrile between 69 and 112°K (J.-T. Wang and F. Williams, unpublished work). The experimental rate constants can be compared with the values predicted by the present model for a gaussian barrier with the parameters V_0 = 10.5 kcal/mol, β = 29.6, and $A = 9 \times 10^{13}$ sec^{-1}. At 69°K, $k_{exp} = 1.02 \times 10^{-2}$ min^{-1} ($k_{cal} = 0.75 \times 10^{2}$ min^{-1}); at 100°K, k_{exp} = 0.225 min^{-1} (k_{cal} = 0.203 min^{-1}); and at 112°K, k_{exp} = 0.99 min^{-1} (k_{cal} = 0.89 min^{-1}). The agreement is very satisfactory considering that $\Gamma(T)$ changes by almost 11 orders of magnitude over this temperature range, and that an uncertaintainty of a power of 10 in A is allowed by the treatment (see eq 5 and Figure 3).

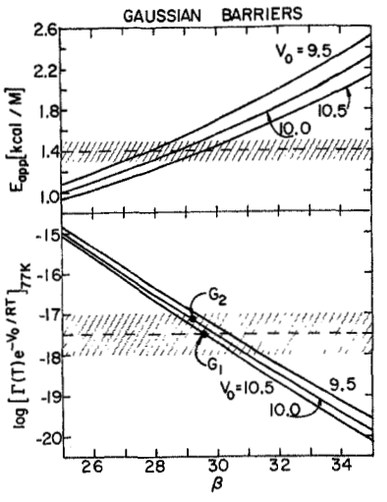

Figure 3. As in Figure 1, for gaussian barriers (see eq 8).

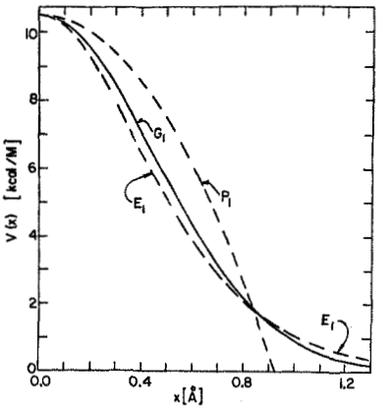

Figure 4. Potential barriers corresponding to points P_1, E_1, and G_1 on Figures 1–3, respectively, (see Table I); only positive values of x are shown since all the barriers considered are symmetric about $x = 0$.

V_0, β (or a), and the barrier shape (parabolic, Eckart, or gaussian). The only additional contributing evidence is the fact that the width scaling parameter of the optimal (gaussian) barrier G_1, $a = 0.636$ Å, is a plausible result in that it is very similar to values obtained for barriers corresponding to a number of other H-atom transfer reactions (*e.g.*, see Table VII in ref 5).[13]

On the other hand, the present work does demonstrate that the high-temperature gas-phase and low-temperature solid-phase rate constants may be quantitatively explained in terms of a single potential energy surface. This presents a much simpler picture of the reacting system than would arise if one had to try to estimate changes in the potential energy surface between the gas and solid phases. Furthermore, the small differences between the high-temperature gas-, and low-temperature solid-phase values of the divers vibrational frequencies of acetonitrile[10] strongly suggests that any such changes would be quite small. In addition, the conclusion that the low-temperature reaction occurs almost completely *via* quantum-mechanical tunneling suggests that the validity of the present picture may be cleanly tested by comparing the predicted isotope effects (see Figure 5) with experiment. However, such measurements are in practice very difficult to perform because of the very slow rate of the corresponding deuterium abstraction process.

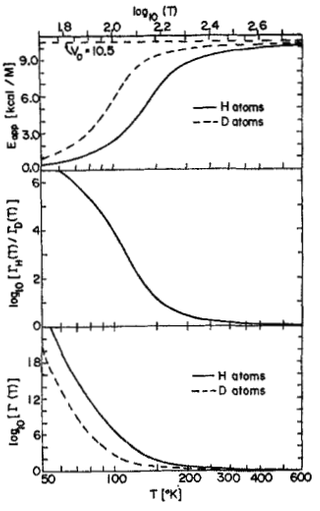

Figure 5. Temperature dependence and tunneling factors for reaction 1 occurring with H or D atoms being transferred; these were calculated for the gaussian potential barrier G_1 (see Table I).

Acknowledgment. We are very grateful to Professor J. E. Willard and Dr. J. R. Miller for making us cognizant of our common interest in this problem.

Appendix

On Calculating the Permability of One-Dimensional Potential Barriers. Recently a numerical method was presented for calculating exact tunneling probabilities for arbitrary finite one-dimensional potential barriers.[12,14,15] The purpose of the present discussion is to describe a simple addition to the numerical method of ref 12 (hereafter denoted LQL) which allows a saving in computation time and removes any uncertainty about the convergence of the solution. The procedure is to introduce a WKB "edge-effect" correction to the phases and amplitudes of the numerical wavefunctions at the two boundaries. Throughout, familiarity with LQL[12] and the definitions given therein are assumed,[16] and equation numbers from there are prefixed by LQL.

(13) Although the results in Table VII of ref 5 were obtained using truncated parabola potential barriers [eq 7], the range of values reported, $0.48 \leq a \leq 0.83$ Å, should give a fairly realistic measure of barrier width.

(14) A method similar to that of ref 12 was previously used in a study of the Schottky effect;[15] however, these authors were utilizing semi-infinite potentials and did not consider "edge effect" corrections of the type discussed here.

(15) G. G. Belford, A. Kuppermann, and T. E. Phipps, *Phys. Rev.*, **128**, 524 (1962).

The tunneling probability calculation outlined by eq LQL 1-7 is exact as long as the numerical integration to yield the function $\phi_1(y)$ and $\phi_2(y)$ is performed over the entire interval between the boundary regions where they are exactly described by eq LQL 5 and LQL 6. However, for realistically smooth potentials this interval is infinite, and this requirement cannot be precisely satisfied. In the test calculations of LQL this difficulty was circumvented by assuming the validity of eq LQL 5-7 at the ends of a chosen finite interval, and then increasing the length of the interval until it had no significant further effect on the computed permeability, $\kappa(\bar{E})$. It was found that this condition could be quantitatively expressed as a restriction on the value of the WKB convergence criterion at the chosen boundaries

$$\left| [\alpha(y)]^{-2} \frac{d\alpha(y)}{dy} \right| \leq Z \tag{A1}$$

where $Z \sim 1.0 \times 10^{-5}$. The present treatment presents versions of eq LQL 5-7 which are appropriate when the potential is not identically zero at the ends of the chosen interval. Their utilization allows a weakening of the restriction represented by eq A1 [*i.e.*, an increase in the allowed value of Z], which may save considerable computation time.

Examination of first-order WKB wave functions[17] shows that at large and positive, but finite y (where $\alpha(y) > 0$), the $y \simeq +\infty$ solutions described by eq LQL 5 become

$$\begin{aligned} \phi_1(y) &= A_T \left[\frac{\alpha_+}{\alpha(y)}\right]^{1/2} \cos [\alpha_+ y + \delta_+(y)] \\ \phi_2(y) &= A_T \left[\frac{\alpha_+}{\alpha(y)}\right]^{1/2} \sin [\alpha_+ y + \delta_+(y)] \end{aligned} \tag{A2}$$

where

$$\delta_+(y) = \int_y^\infty [\alpha_+ - \alpha(x)]\, dx \tag{A3}$$

Similarly, the solutions at large negative y (where $\alpha(y) > 0$), which in the $y \simeq -\infty$ limit become eq LQL 6, are

$$\begin{aligned} \phi_1(y) &= \left[\frac{\alpha_-}{\alpha(y)}\right]^{1/2} \{C_1 \cos [\alpha_- y + \delta_-(y)] + \\ &\qquad D_1 \sin [\alpha_- y + \delta_-(y)]\} \\ \phi_2(y) &= \left[\frac{\alpha_-}{\alpha(y)}\right]^{1/2} \{C_2 \cos [\alpha_- y + \delta_-(y)] + \\ &\qquad D_2 \sin [\alpha_- y + \delta_-(y)]\} \end{aligned} \tag{A4}$$

where

$$\delta_-(y) = -\int_{-\infty}^y [\alpha_- - \alpha(x)]\, dx \tag{A5}$$

As before, the permeability may be expressed directly in terms of values computed for the solution functions $\phi_1(y)$ and $\phi_2(y)$ at the integration mesh points y_1 and y_2 (large and negative). However, the inclusion of the phase, $\Delta(y_2,y_1) \equiv \delta_-(y_2) - \delta_-(y_1)$, and amplitude, $A(y) \equiv [\alpha_-/\alpha(y)]^{1/2}$, factors modifies eq LQL 7, yielding

$$\begin{aligned} \kappa(\bar{E}) = 4(\alpha_+/\alpha_-)\{ & A(y_1)A(y_2) \sin [\alpha_-(y_2 - y_1) + \\ & \Delta(y_2,y_1)]\}^2 |A_T|^2 \times \{[A(y_2)\phi_1(y_1)]^2 + [A(y_2)\phi_2(y_1)]^2 + \\ & [A(y_1)\phi_1(y_2)]^2 + [A(y_1)\phi_2(y_2)]^2 - 2[\phi_1(y_1)\phi_1(y_2) + \\ & \phi_2(y_1)\phi_2(y_2)]A(y_1)A(y_2) \cos [\alpha_-(y_2 - y_1) + \Delta(y_2,y_1)] + \\ & 2[\phi_1(y_1)\phi_2(y_2) - \phi_1(y_2)\phi_2(y_1)]A(y_1)A(y_2) \sin [\alpha_-(y_2 - \\ & y_1) + \Delta(y_2,y_1)]\}^{-1} \end{aligned} \tag{A6}$$

Another way of expressing the change from eq LQL 7 to eq A6 is to multiply the former by $[A(y_1)A(y_2)]^2$, add $\Delta(y_2,y_1)$ to the arguments of the trigonometric functions, and replace $\phi_i(y_1)$ by $\{A(y_2)\phi_i(y_1)\}$ and $\phi_i(y_2)$ by $\{A(y_1)\,\phi_i(y_2)\}$ $[i = 1, 2]$. While the amplitude factors $[\alpha_+/\alpha(y)]^{1/2}$ and $[\alpha_-/\alpha(y)]^{1/2}$ are adequately defined as stated, the phase correction factors $\delta_+(y)$ and $\delta_-(y)$ [and hence $\Delta(y_2,y_1)$] depend on the nature of the particular potential barrier $\bar{V}(y)$, and their properties are discussed below. An initial observation is that for barriers symmetric about $y = 0$: $\delta_-(-|y|) = -\delta_+(|y|)$.

The following discussion assumes, without loss of generality, that at each asymptote ($y \simeq +\infty$ or $-\infty$) the zero of energy is chosen such that $V(y) \to 0$ at these limits. In this case, eq A3 and A5 may be written as

$$\begin{aligned} \delta_+(|y|) &= \alpha_+ \int_{|y|}^\infty [1 - (1 - \bar{V}(x)/\bar{E})^{1/2}]\, dx \\ \delta_-(-|y|) &= -\alpha_- \int_{-\infty}^{-|y|} [1 - (1 - \bar{V}(x)/\bar{E})^{1/2}]\, dx \end{aligned} \tag{A7}$$

If $|y|$ is chosen sufficiently large that $|\bar{V}(x)/\bar{E}| \ll 1$ for all $|x| > |y|$, it is clearly valid to expand the integrands of eq A7 as Taylor's series, and retaining only the leading term[18]

$$\begin{aligned} \delta_+(|y|) &\approx (\alpha_+/2\bar{E}) \int_{|y|}^\infty \bar{V}(x)\, dx \\ \delta_-(-|y|) &\approx (-\alpha_-/2\bar{E}) \int_{-\infty}^{-|y|} \bar{V}(x)\, dx \end{aligned} \tag{A8}$$

For typical analytic potentials eq A8 are readily in-

(16) The LQL[12] quantity of most relevance to the present discussion is $\alpha(y) = (\beta/\pi)\,[\bar{E} - \bar{V}(y)]^{1/2}$, where $y = x/a$, β is the dimensionless parameter of eq 9 and $\bar{E}$ and $\bar{V}(y)$ are, respectively, the incident particle energy and the potential function, both scaled by the barrier height V_0. Note that $\alpha(+\infty) \equiv \alpha_+$ and $\alpha(-\infty) \equiv \alpha_-$.

(17) See, *e.g.*, E. Merzbacher, "Quantum Mechanics," Wiley, New York, N. Y., 1961, Chapter 7.

(18) In numerical checks against the exact analytic tunneling probabilities for Eckart barriers it was found that inclusion of the next term in this expression did not significantly improve the results.

(19) M. Abramowitz and I. A. Stegun, "Handbook of Mathematical Functions," National Bureau Standards, Applied Math Series, No. 55, U. S. Dept. of Commerce, 1964, §7.1.

tegrable. For an Eckart function, $\bar{V}(y) = 1/\cosh^2(y)$, it yields

$$\delta_+(|y|) = \alpha_+/[\bar{E}(e^{|2y|} + 1)] = -\delta_-(-|y|)$$

while for a gaussian barrier, $\bar{V}(y) = e^{-y^2}$, it yields

$$\delta_+(|y|) = \pi^{1/2}\alpha_+ \operatorname{erfc}(y)/4\bar{E} = -\delta_-(-|y|)$$

where erfc(y) is the well known error function.[19] Analogously simple expressions for the phase shifts are readily obtained for other model barriers.

Using the above results, the "WKB-improved" permeability calculations would proceed precisely as before except that eq A2 replaces eq LQL 5 as the source of the starting values of the wave function used in initiating the numerical integration, and eq A6 replaces eq LQL 7 as the source of $\kappa(\bar{E})$. Of course a subroutine would have to be added to the computer program to supply the values of $\delta_+(y)$ and $\delta_-(y)$ appropriate to the asymptotic form of the given potential. Testing this approach with Eckart barriers of different sizes (for which exact $\kappa(\bar{E})$ values are known analytically), it was found that the inclusion of these corrections allows a given accuracy in $\kappa(\bar{E})$ to be achieved using a value of Z [see eq A1] one order of magnitude larger than before. For example, $\kappa(\bar{E})$ could be obtained accurate to 1×10^{-5} using $Z = 1 \times 10^{-4}$, while LQL had found that $Z = 1 \times 10^{-5}$ was required.

One additional improvement in the present computer program over that used by LQL is the addition of a capability for changing the integration mesh in the course of a calculation. Including this and the edge-effect corrections may lead to a considerable saving in computation time. However, this would probably be relatively more important for potentials which die off at long range with an inverse-power form, than for the exponential-tailed potentials considered here. Annotated FORTRAN listings of the computer programs used in the present calculations are available from the first author (R. J. L.)

The Role of Nonbonded Intramolecular Forces in Barriers to Internal Rotation in Molecules with Two Equivalent Methyl Groups

by Kenneth C. Ingham

Department of Biophysics, Michigan State University, East Lansing, Michigan 48823 *(Received September 9, 1971)*

Publication costs borne completely by The Journal of Physical Chemistry

It is suggested that the often large barrier difference between molecules with two equivalent methyl groups and their corresponding one-top analogs can be readily explained on the basis of a nonbonded repulsion between the methyl groups. The repulsion arises primarily from an interaction between the protons of one methyl group and the carbon atom of the other. This dominance of the H···C interactions offers a simple explanation of the general success of the independent oscillator approximation in most of these two-top molecules.

A recent study of hindered internal rotation in *o*-xylene generated interest in the role of nonbonded (van der Waals) forces in barriers to internal rotation in two-top molecules.[1,2] A survey of available data revealed that molecules containing two equivalent neighboring methyl groups often have rotational barriers whose magnitudes differ substantially from those of their corresponding one-top analogs, for example, dimethyl ether *vs.* methanol (see Table I). Yet, the independent oscillator approximation, which assumes that each methyl group oscillates in a potential well whose shape is independent of the orientation of the other methyl group, is generally a fairly good approximation in these molecules. These observations could be made compatible by postulating a strong repulsive interaction between the hydrogen atoms of one methyl group and the carbon atom of the other.

In order to check this hypothesis a variety of nonbonded potential functions were tested for their ability to explain the *difference* in barrier between the two-top molecules and their one-top analogs. The calculation is similar to that used by others[3,4] to explain the effect

(1) K. C. Ingham, Ph.D. Thesis, University of Colorado, 1970.

(2) K. C. Ingham and S. J. Strickler, *J. Chem. Phys.*, **53**, 4313 (1970).

(3) J. L. DeCoen, G. Elefante, A. M. Liquori, and A. Damiani, *Nature (London)*, **216**, 910 (1967).

(4) R. Scott and H. Scheraga, *J. Chem. Phys.*, **42**, 2209 (1965).